AIAA JOURNAL
Vol. 46, No. 7, July 2008

Modal Identification of Truss Structures by Changing Stiffness Using Piezoelectric Actuator

Atsuhiko Senba*
Nagoya University, Nagoya, Aichi 464-8603, Japan
and
Kaoru Ohashi† and Hiroshi Furuya‡
Tokyo Institute of Technology, Yokohama, Kanagawa 226-8502, Japan

DOI: 10.2514/1.35272

This study proposes a modal identification technique for truss structures by changing the stiffness using a piezoelectric actuator. The technique is formulated on the basis of the vibration characteristics of truss structures with a metal-sealed-type multilayer piezoelectric actuator installed in a specific truss member. The natural frequency of the truss is changed by the stiffness control of a truss member to identify the natural frequency of the truss structure; the axial stiffness of the truss member can be semi-actively controlled using piezoelectric materials and an electrical circuit. The frequency response amplitude is changed by the change of stiffness of the truss, then the change ratio of the frequency response amplitude can be used to identify the natural frequency of the truss, and then the excitation data are not required to be measured. The method is appropriate for the identification of space structures in orbit in the case when excitation data are not fully available because of unknown excitation forces and disturbances. Experimental demonstrations of the identification of the first bending modal frequency of a 10-bay truss with a piezoelectric actuator are presented. It is found that the estimated natural frequency is in good agreement with the exact frequency, even though excitation force data are not provided. Furthermore, the factors causing the identification error are discussed through theoretical sensitivity analyses. The results show that the identification error can be reduced when the frequency response amplitude of a specific excitation frequency derived from the natural frequency is used for the identification.

Nomenclature

$\mathbf{B}_p$	=	input matrix
b_p	=	piezoelectric constant
$\mathbf{C}$	=	damping matrix
$\mathbf{C}_p$	=	diagonal capacitance matrix
C_p	=	capacitance of actuator
c_r	=	rth modal damping
F_i	=	excitation force
$\mathbf{f}$	=	external force vector
f_p	=	tensile force exerted on actuator
$\hat{H}_{rij}$	=	frequency response amplitude for high stiffness
H_{rij}	=	frequency response amplitude for low stiffness
$\mathbf{K}$	=	stiffness matrix
k_p	=	constant-charge stiffness
k_r	=	rth modal stiffness
$\mathbf{M}$	=	mass matrix
$\hat{m}_r$	=	rth modal mass for high stiffness
m_r	=	rth modal mass for low stiffness
N	=	number of different excitation frequency
n	=	number of degrees of freedom
$\mathbf{Q}$	=	electrical charge vector
Q	=	electrical charge applied to actuator
R_j	=	$\hat{H}_{\kappa ij}/H_{rij} - 1$
R_Ω	=	$\hat{\Omega}_1^2/\Omega_1^2$
$\mathbf{V}_p$	=	voltage vector
V_p	=	voltage
$\hat{X}_{ij}$	=	stationary amplitude for high stiffness
X_{ij}	=	stationary amplitude for low stiffness
$\mathbf{x}$	=	displacement vector
x_p	=	displacement of actuator
Δk	=	variation of modal stiffness
Δk_p	=	variation of stiffness of a piezoelectric actuator
Δm	=	variation of modal mass
$\partial\{\cdot\}/\partial\{\cdot\}$	=	partial derivative
$\hat{\zeta}_r$	=	rth damping ratio for high stiffness
ζ_r	=	rth damping ratio for low stiffness
$\hat{\phi}_r$	=	rth mode shape for high stiffness
ϕ_r	=	rth mode shape for low stiffness
$\hat{\Omega}_r$	=	rth natural frequency for high stiffness
Ω_r	=	rth natural frequency for low stiffness
ω	=	excitation frequency
ω_1	=	first resonance frequency for high stiffness
ω_2	=	first resonance frequency for low stiffness
$\bar{\omega}_1, \bar{\omega}_2$	=	two extrema of R_j

Subscripts

i	=	ith node of truss
j	=	jth node of truss
r	=	rth mode

Superscripts

T	=	matrix transpose
-1	=	matrix inverse
$*$	=	value before mass variation

Received 23 October 2007; revision received 12 February 2008; accepted for publication 21 February 2008.

*Assistant Professor, Department of Information Engineering, Furo-cho, Chikusa-ku. AIAA Member.

†Undergraduate Student, Department of Mechano-Aerospace Engineering, 2-12-1 Ookayama, Meguro-ku, Tokyo 152-8550.

‡Associate Professor, Department of Built Environment, Nagatsuta 4259-G3-6, Midori-ku, Yokohama 226-8502. AIAA Senior Member.

I. Introduction

THE identification of modal parameters, such as the natural frequency, damping ratio, and mode shapes of structural systems, generally requires both input and output data obtained by

sensors in structures [1,2]. There are many studies on structural system identification and vibration-based structural damage detection that have evaluated the stiffness parameters of structures with potential damages [3].

The identification of the modal parameters of space structures in orbit has become important, as these structures have become large and highly flexible for use in advanced space missions that employ large flexible antennas, reflectors, and solar arrays. System identification using active members used as vibration exciters in truss structures has been studied by Chen and Fanson [4]. Further, damage assessment using vibration data has been investigated by Chen and Garba [5]. Kammer has proposed a method for sensor placements for the on-orbit modal identification of large space structures [6]. Practical identification experiments on the Hubble Space Telescope have been reported by Anthony and Anderson [7]. Further, Adachi et al. have performed the on-orbit identification experiments on the Japanese engineering test satellite ETS-VI [8]. Kammer and Stelzner have analyzed the possibility of the structural identification of Mir/shuttle docking data using inverse system dynamics [9].

In particular, the on-orbit identification of future space structures is a challenging task because measuring the exact excitation force acting on structures, and also the disturbance or ambient excitation affecting them, is not always feasible in orbit [10]. Various excitation sources exist for large space structures such as space stations, and these excitations are often periodic and not fully measured in practical cases [11]. For example, thermal excitation, rotary joints of solar arrays, gyros for attitude control, thermal radiators, and fluid pumps have been observed to cause disturbance in spacecraft [7,10]. However, their models of the frequency distribution and force may not be realized accurately, although the force acting on the spacecraft can be assumed to be random, stationary, or transient. Therefore, methods that do not require the measurement of these input excitation forces are necessary for achieving a reliable on-orbit identification of large space structures.

The issue of modal identification by using output-only data has been investigated in recent studies on civil engineering structures, such as buildings and bridges, because they are frequently excited by wind loading and traffic loading, which cannot be measured easily [12]. The identification using output-only data can be theoretically possible when a purely impulsive force or white noise is applied to the structures, because the resulting output data in these cases can be regarded as the impulse response data or random excitation data of the structural systems. Then, it would be possible to use various types of conventional system identification algorithms such as the eigensystem realization algorithm and subspace identification methods [13,14]. Frequency domain approaches have been developed by McKelvey et al. [15] and Pintelon et al. [16]. However, the output data for sinusoidal excitation forces with an unmeasurable amplitude cannot be directly analyzed by these methods.

On the other hand, Goodzeit and Phan have proposed a method for the system identification in the presence of unknown periodic disturbances [17]. The measurements of only the excitation control input and the disturbance-contaminated response data are used for the system identification. Further, Brincker et al. have proposed a frequency domain technique for modal parameter identification with output-only measurement [18]. They have used the singular value decomposition of the spectral density function matrix. Antoni et al. have investigated the performance of some methods proposed for output-only data and pointed out the difficulty in discriminating system modes and additive noise [19]. In their study, they have also proposed two improved techniques. One uses the difference between the envelopes of a pure deterministic sinusoidal signal and a random signal, and the other uses the difference between the correlation functions of a sinusoidal and random signal. A time-domain method based on singular value decomposition has been proposed by Kim et al. [20]. Lu and Law have proposed an iterative method for identifying system parameters and the input force acting on structures under the assumption that the input location is known [21]. Vibration-based structural health monitoring using output-only measurements has been investigated by Deraemaeker et al. [22] by stochastic subspace identification. These studies on the identification using output-only measurement may have a limitation on their validity in space because of their theoretical assumptions. The following assumptions cannot always be made: a signal for excitation control is available [17], an unknown excitation force is considered as white noise [12], and the location of excitation is accurately known [21]. If the structures are subject to sinusoidal excitation of an unknown amplitude and the location of the excitation force is also unknown, alternative approaches are requested; therefore, this study addresses this issue. In addition, the disturbances whose frequency is close to the lower natural frequency of the structure has attracted a lot of attention in conventional studies, because one of the purposes of modal identification is to use the results for designing the control model necessary for vibration suppression.

Structural mass, stiffness, and damping parameters are also identified by vibration data. However, in some cases, some of the structural parameters such as stiffness are difficult to identify because of measurement noise, lack of sensitivity of modal data with respect to specific parameters, and lack of controllability of excitation sources. Because of ill-conditioned problems in the inverse calculation for the identification of structural parameters, nonunique solutions are obtained. In particular, for the identification of structural damages, the sensitivity should be enhanced by some additional approaches to improve the accuracy of the determination of both the location and extent of damages. To overcome these problems, many researchers have proposed improved vibration testing methods that are mainly developed for damage detection. The sensitivity-enhancing control (SEC) technique developed by Ray and Tian [23] uses a feedback control system in structures to improve the sensitivity of modal properties with respect to the change in the local stiffness or mass parameters. Similar approaches have been developed by Lew [24] using a virtual passive controller, and by Jung and Park [25]. Solbeck and Ray have investigated the feasibility of the SEC technique through damage detection experiments performed by adopting a coherence approach [26]. Jiang et al. have proposed tunable piezoelectric transducer circuitry with a controllable inductance for damage detection, and they have demonstrated an improvement in the accuracy of damage identification through numerical experiments on a cantilevered beam [27]. The authors have proposed the concept of self-identification using variable structural parameters in adaptive structure systems [28,29]. In these studies, the relationship between modal properties and a geometric parameter, such as the angle of truss members in a variable geometry truss (VGT), is used for increasing the amount of modal information to identify the stiffness matrix of the VGT. An experimental study on the parameter identification of a flexible beam has been carried out using variable-inertia systems on the basis of an extended form of the variable matrices method [28] using the self-identification concept [30].

In the field of adaptive structures, the controllable and adaptive structural properties of embedded smart materials and active members in structural systems have been comprehensively investigated [31,32]. For example, the active control of stiffness by piezoelectric actuators for the vibration suppression of truss structures has been studied by Onoda et al. [33]. They have used a piezoelectric actuator for changing the axial stiffness of the truss member so that the vibration energy can be dissipated effectively. Makihara et al. have proposed the method of semi-active vibration suppression by recycling energy by using a piezoelectric actuator with electrical circuitry, in which the stiffness of the truss members is controlled semi-actively by switching the circuit on the basis of an optimal control law [34,35].

Although the active control of piezoelectric actuators has been successfully used to improve the vibration suppression, such stiffness control, particularly for modal identification, has not yet been studied. Active and semi-active vibration suppressions usually employ the state space models of the structure for effectively switching the electrical circuit of the piezoelectric actuator on the basis of the linear quadratic regulator (LQR) control theory [36]. The state-space model must be sufficiently accurate to calculate the

optimal control gain of the LQR. However, for large space structures in orbit, their phased construction and docking event, and the deployment of flexible components such as mesh antennas, can vary the natural frequency of the structures considerably; therefore, the natural frequency must be identified in orbit.

When the identification of such structures can be realized by piezoelectric actuators that are also used as devices for vibration suppression, more reliable and adaptable identification and vibration suppression systems can be realized; therefore, the method for the identification using piezoelectric devices is very important for both identification and vibration suppression. Therefore, we study a method for identifying modal parameters by using piezoelectric devices, under the condition that only the frequency response amplitude is available, by assuming that the structure has variable-stiffness active members.

The purpose of the present study is to investigate the possibility of modal identification on the basis of the frequency response amplitude of structures; here, the semi-active stiffness control of truss structures is used so that input force data are not required for the identification. The frequency response amplitude of structures with variable-stiffness devices can be changed by changing stiffness. Further, it is assumed that the change ratio of the frequency response amplitude is a function of unknown modal parameters. We therefore investigate the possibility of updating the natural frequency on the basis of the change ratio of the frequency response amplitude. In particular, we focus on the use of piezoelectric devices for changing the stiffness of a member in truss structures.

In this paper, we first explain the vibration characteristics of variable-stiffness structures with piezoelectric devices. Then, the concept and method of identification using the change ratio of the frequency response amplitude are described. Finally, we show some experimental results of modal parameter identification for a 10-bay truss structure to demonstrate the proposed method. The identification error is also discussed.

II. Dynamic Characteristics of Truss Structures with Piezoelectric Devices

We first explain the vibration characteristics of truss structures with piezoelectric devices. The piezoelectric device employed in this study is a metal-sealed-type multilayer piezoelectric actuator. It converts electrical energy into a form of mechanical energy, such as displacement. We use NEC TOKIN's commercially available multilayer piezoelectric actuator as a member of the truss structure, in which the axial stiffness of the truss members is controlled piezoelectrically to identify the fundamental natural frequency of the truss. Figure 1 shows the photograph of the piezoelectric actuator used in this study.

A. Properties of Piezoelectric Device as Truss Member

The piezoelectric transducer is embedded in one of the members of the truss. Because a similar piezoelectric device has been studied in literature, we provide a summary of its properties and configuration here. Interested readers may consult [36] for the detailed description of this device. According to [34,36], the relationship among the tensile force f_p, axial displacement x_p, electrical charge of capacitor Q, and voltage V_p between two terminals of the piezoelectric device can be expressed as

$$f_p = k_p x_p - b_p Q \quad \text{and} \tag{1}$$

$$V_p = -b_p x_p + Q/C_p \tag{2}$$

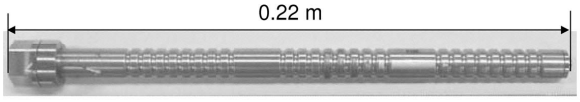

Fig. 1 Photograph of metal-sealed-type multilayer piezoelectric actuator embedded in truss member (NEC/TOKIN: ASB171C801NP0).

where k_p, b_p, and C_p are the constant-charge spring constant, piezoelectric constant of the piezoelectric transducer, and capacitance of the piezoelectric transducer, respectively. Eliminating Q from Eqs. (1) and (2), the following equation is obtained:

$$f_p = \left(k_p - b_p^2 C_p\right) x_p - b_p C_p V_p \tag{3}$$

Equation (3) represents the principle of the stiffness change of a piezoelectric device: when one shunts the two terminals, that is, by substituting $V_p = 0$ into Eq. (3), the spring constant becomes $k_p - b_p^2 C_p$ and Eq. (3) can be rewritten as

$$f_p = \left(k_p - b_p^2 C_p\right) x_p \tag{4}$$

On the other hand, when one opens the terminals, that is, by substituting Q (=const.) into Eq. (1), the spring goes into the high-stiffness state, and Eq. (1) becomes independent of V_p in Eq. (2) as

$$f_p = k_p x_p + \text{const.} \tag{5}$$

Thus, two different stiffness states of the truss member, as shown in Eqs. (4) and (5), are available by a simple shunting switch of the circuit. In [36], vibration suppression is also carried out by the same type of actuator; however, the stiffness is changed repeatedly on the basis of the LQR control law, according to the vibration to be dissipated. In contrast, for identification, the stiffness should be maintained as either high or low during data acquisition for measuring the frequency response amplitude in each state.

B. Equation of Motion for a Truss Structure

The equation of motion for truss structures with a piezoelectric device can be derived by considering the coupling of the displacement of the truss nodes and the voltage between the two terminals of the piezoelectric device [36].

$$\mathbf{M}\ddot{\mathbf{x}} + \mathbf{C}\dot{\mathbf{x}} + \mathbf{K}\mathbf{x} = \mathbf{f} + \mathbf{B}_p\mathbf{Q} \tag{6}$$

and

$$\mathbf{V}_p = -\mathbf{B}_p^T\mathbf{x} + \mathbf{C}_p^{-1}\mathbf{Q} \tag{7}$$

where $\mathbf{M}$, $\mathbf{C}$, $\mathbf{K}$, $\mathbf{B}_p$, and $\mathbf{C}_p$ are the $(n \times n)$ mass matrix, damping matrix, stiffness matrix, charge input matrix, and diagonal capacitance matrix, respectively. Further, $\mathbf{x}$, $\mathbf{V}_p$, $\mathbf{f}$, and $\mathbf{Q}$ are the $(n \times 1)$ displacement vector, external force vector, voltage vector, and charge vector, respectively.

Equations (6) and (7) show that two different states of the vibration, that is, high-stiffness and low-stiffness states, can be obtained due to the shunting of the circuit of the piezoelectric device. Substituting $\mathbf{V}_p = \mathbf{0}$ into Eq. (7) and eliminating $\mathbf{Q}$ in Eq. (6), we can obtain the relation for the low-stiffness state as

$$\mathbf{M}\ddot{\mathbf{x}} + \mathbf{C}\dot{\mathbf{x}} + \left(\mathbf{K} - \mathbf{B}_p\mathbf{C}_p\mathbf{B}_p^T\right)\mathbf{x} = \mathbf{f} \tag{8}$$

Further, by substituting $\mathbf{Q} = \mathbf{0}$ into Eq. (6), the relation for the high-stiffness state is easily obtained as

$$\mathbf{M}\ddot{\mathbf{x}} + \mathbf{C}\dot{\mathbf{x}} + \mathbf{K}\mathbf{x} = \mathbf{f} \tag{9}$$

We adopt these two relations, Eqs. (8) and (9), to change the frequency response amplitude and to obtain the resulting change ratio for the modal parameter identification, in which the value of the amplitude of the sinusoidal excitation force is not required.

III. Modal Identification of Truss Structure by Changing Stiffness

Figure 2 shows a truss structure in which one member of the truss is a piezoelectric device that can vary its axial stiffness. As described in the previous section, such a truss structure has two different stiffness states; therefore, its natural frequency can also vary. When

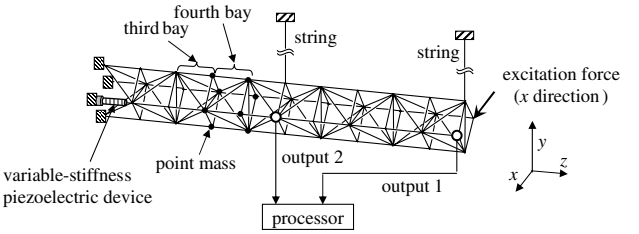

Fig. 2 Ten-bay truss structure for experiments with variable-stiffness piezoelectric device (also see Fig. 1).

the natural frequency can be changed by stiffness control using the piezoelectric device, it is expected that the frequency response amplitude can be changed. Then, it is possible to use the change in the frequency response amplitude to identify modal properties such as the natural frequency of the truss structure. This section proposes identification procedures by using such variable characteristics of the truss, particularly for specific situations in which the characteristics of the excitation force, such as its frequency, amplitude, and location, acting on a structure cannot be measured accurately.

A. Change Ratio of Frequency Response Amplitude

The frequency response function and its change ratio due to the change in stiffness by the piezoelectric device are derived. We transform Eq. (6) into the modal form using modal coordinates. Then, the response amplitude for the high-stiffness and the low-stiffness states can be written as

$$|\hat{X}_{ij}(\omega)| = \left(\sum_{r=1}^{n} \hat{H}_{rij}\right) F_i \tag{10}$$

and

$$|X_{ij}(\omega)| = \left(\sum_{r=1}^{n} H_{rij}\right) F_i \tag{11}$$

respectively, where excitation forces $F_i e^{i\omega t}$ $(F_i > 0)$ are applied in the x direction of the ith node of the truss shown in Fig. 2. Further, the amplitudes $\hat{H}_{rij}$ and H_{rij} for each mode can be written as

$$\hat{H}_{rij} = \frac{\hat{\phi}_{ri}\hat{\phi}_{rj}}{\hat{m}_r\sqrt{(\hat{\Omega}_r^2 - \omega^2)^2 + (2\hat{\zeta}_r\hat{\Omega}_r\omega)^2}} \tag{12}$$

and

$$H_{rij} = \frac{\phi_{ri}\phi_{rj}}{m_r\sqrt{(\Omega_r^2 - \omega^2)^2 + (2\zeta_r\Omega_r\omega)^2}} \tag{13}$$

where $|\hat{X}_{ij}(\omega)|$, $\hat{\Omega}_r$, $\hat{\phi}_r$, $\hat{\zeta}_r$, and $\hat{m}_r$ are the frequency response amplitude of the jth node for the rth mode, undamped natural angular frequency, mode shape, modal damping ratio, and modal mass, respectively, for the high-stiffness states. The corresponding parameters for the low-stiffness state are $|X_{ij}(\omega)|$, Ω, ϕ_r, ζ_r, and m_r. The excitation frequency and the amplitude of the excitation force are ω and $F_i(\omega)$, respectively.

Then, we define the change ratio of the frequency response amplitude using Eqs. (10–13) as

$$R_j \equiv \frac{\hat{H}_{1ij}}{H_{1ij}} - 1 = \sqrt{\frac{(\Omega_1^2 - \omega^2)^2 + (2\zeta_1\Omega_1\omega)^2}{(\hat{\Omega}_1^2 - \omega^2)^2 + (2\hat{\zeta}_1\hat{\Omega}_1\omega)^2}} - 1 \tag{14}$$

where the unknown parameters to be identified are Ω_1 and Ω_1' in Eq. (14). For defining Eq. (14), we assume that the first mode of the truss is dominant (i.e., $r = 1$). Further, the changes in the mode shape and modal mass due to the stiffness control by the piezoelectric device are assumed to be negligible, then $\hat{\phi}_{1i}\hat{\phi}_{1j} = \phi_{1i}\phi_{1j}$ and $\hat{m}_1 = m_1$. Of course, theoretically, the mode shape would depend on the stiffness; however, it is known, in literature, that the change in mode shapes for the first bending mode of truss structures by the local stiffness change is sufficiently small [37]. For the damage detection, using the modal data of lower vibration modes can be often affected by the low sensitivity of the mode shapes. The lack of the sensitivity of the mode shape with respect to the local stiffness variation is not ideal for the purpose of damage detection, whereas it is ideal for the approximation as Eq. (14).

The change ratio R_j can also be defined as $\hat{H}_{1ij}/H_{1ij}$, i.e., without the "-1" terms of Eq. (14). However, Eq. (14) may clearly indicate that when the change in the frequency amplitude is zero, both sides of Eq. (14) are also zero.

It should be noted that specific structures with high-modal density should consider multiple vibration modes for deriving Eq. (14). The high-modal density can be defined such that the natural frequencies of multiple modes are very close. For the case of high-modal density, the contribution of the multiple modes cannot be neglected; therefore, the change ratio of the frequency response amplitudes should be a function of multiple modes, otherwise, the approximation is inaccurate. Further, unknown variables in the change ratio increases for the case of the high-modal density, then the estimation of the natural frequency is more complicated. However, this study focuses attention on the first mode because the first mode is well separated for various beamlike structures.

B. Estimation Algorithm of Natural Frequency

Thus far, the change ratio of the frequency response amplitude for formulating the identification method by the stiffness control using a piezoelectric device has been defined by Eq. (14). This section presents an algorithm for identifying the natural frequency of the truss structure that is subject to unknown sinusoidal excitation.

1. Assumptions

To describe the formulation of the identification algorithm, we should first assume that the mass varies in on-orbit due to docking, the refueling process, and so on. The stiffness can also vary in orbit by structural damages and repair, or the deployment of flexible components such as solar arrays. Because all cases cannot be fully covered in this study, we address specific cases where the natural frequency is changed by the change in the mass in orbit. It should be noted that the first modal damping ratio ζ_1, the natural frequencies for the high- and low-stiffness states before the mass variation, are assumed to be provided before the identification of $\hat{\Omega}_1$ and Ω_1.

Suppose that the first modal mass before structural mass variation is m_1 and its variation is Δm; the first modal stiffness is k_1 and its variation by changing stiffness using the piezoelectric actuator is Δk. Then, the first natural frequencies before the mass variation for the high- and low-stiffness states can be written as

$$\hat{\Omega}_1^* = \sqrt{\frac{k_1 + \Delta k}{m_1}} \tag{15a}$$

and

$$\Omega_1^* = \sqrt{\frac{k_1}{m_1}} \tag{15b}$$

respectively. On the other hand, the first natural frequencies after mass variation for the high- and low-stiffness states can be written as

$$\hat{\Omega}_1 = \sqrt{\frac{k_1 + \Delta k}{m_1 + \Delta m}} \tag{16a}$$

and

$$\Omega_1 = \sqrt{\frac{k_1}{m_1 + \Delta m}} \tag{16b}$$

respectively. Hence, the following relation is derived from Eqs. (15) and (16) as

$$\frac{\hat{\Omega}_1^{*2}}{\Omega_1^{*2}} = \frac{\hat{\Omega}_1^2}{\Omega_1^2} = \frac{k_1 + \Delta k}{k_1} \equiv R_\Omega \tag{17}$$

2. Estimation of Natural Frequency

Then, let us assume that the experimental value of $\tilde{R}_j$ is given by the two frequency response amplitudes $\hat{H}_{1ij}$ and H_{1ij} for the high- and low-stiffness states under sinusoidal excitation with frequency ω:

$$\tilde{R}_j = \hat{H}_{1ij}/H_{1ij} - 1 = \sqrt{\frac{(\Omega_1^2 - \omega^2)^2 + (2\zeta_1\Omega_1\omega)^2}{(\hat{\Omega}_1^2 - \omega^2)^2 + (2\hat{\zeta}_1\hat{\Omega}_1\omega)^2}} - 1 \tag{18}$$

Further, the relation $\hat{\zeta}_1\hat{\Omega}_1 = \zeta_1\Omega_1$ is obtained because the first modal damping ratio and natural frequency can be expressed as

$$\hat{\zeta}_1\hat{\Omega}_1 = \frac{c_1}{2\sqrt{m_1(k_1 + \Delta k)}}\sqrt{\frac{k_1 + \Delta k}{m_1}} = \frac{c_1}{2m_1} \tag{19a}$$

and

$$\zeta_1\Omega_1 = \frac{c_1}{2\sqrt{m_1 k_1}}\sqrt{\frac{k_1}{m_1}} = \frac{c_1}{2m_1} \tag{19b}$$

where c_1 is the first modal damping coefficient, which is a constant parameter. Then, eliminating $\hat{\zeta}_1$ using $\hat{\zeta}_1\hat{\Omega}_1 = \zeta_1\Omega_1$, Eq. (18) can be rewritten as

$$\tilde{R}_j = \sqrt{\frac{(\Omega_1^2 - \omega^2)^2 + (2\zeta_1\Omega_1\omega)^2}{(\hat{\Omega}_1^2 - \omega^2)^2 + (2\zeta_1\Omega_1\omega)^2}} - 1 \tag{20}$$

Eliminating $\hat{\Omega}_1$ from Eq. (20) using Eq. (17) (i.e., $\hat{\Omega}_1 = R_\Omega\Omega_1$), Eq. (18) is rewritten as

$$\tilde{R}_j = \sqrt{\frac{(\Omega_1^2 - \omega^2)^2 + (2\zeta_1\Omega_1\omega)^2}{(R_\Omega^2\Omega_1^2 - \omega^2)^2 + (2\zeta_1\Omega_1\omega)^2}} - 1 \tag{21}$$

Finally, Eq. (21) can be solved for Ω_1 by substituting $\tilde{R}_j$, R_Ω, ω, and ζ_1 as

$$\Omega_1 = \sqrt{\frac{-b \pm \sqrt{b^2 - ac}}{a}} \tag{22}$$

where constants a, b, and c are expressed by the following equations:

$$a = R_\Omega^2(\tilde{R}j + 1)^2 - 1 \tag{23a}$$

$$b = \{1 - R_\Omega(\tilde{R}j + 1)^2 + 2\zeta_1^2[R_\Omega(\tilde{R}j + 1)^2 - 1]\}\omega^2 \tag{23b}$$

$$c = \left(\tilde{R}_j^2 + 2\tilde{R}_j\right)\omega^4 \tag{23c}$$

respectively.

Thus, the two candidate values for the natural frequency Ω_1 for the low-stiffness state can be calculated using Eq. (22). Of course, one of the candidate values does not satisfy the exact solution. Therefore, a procedure for selecting the correct value is required.

Next, we describe the algorithms for selecting the correct value from the two candidate values given from Eq. (22). To this end, we consider the derivatives of the frequency response amplitudes, $\hat{H}_{1ij}$ and H_{1ij}, and that of the change ratio of frequency response amplitude R_j with respect the excitation frequency ω.

Because we assumed that the first mode is dominant, i.e., $n = 1$ in Eqs. (10) and (11), the sensitivities of $\hat{H}_{1ij}$ and H_{1ij} with respect to ω are derived by differentiating the right-hand sides of Eqs. (12) and (13) with ω:

$$\frac{\partial\hat{H}_{1ij}}{\partial\omega} = \frac{2\hat{\phi}_{1i}\hat{\phi}_{1j}\{\hat{\Omega}_1^2(1 - 2\hat{\zeta}_1^2) - \omega^2\}}{\hat{m}_1\{(\hat{\Omega}_1^2 - \omega^2)^2 + (2\hat{\zeta}_1\hat{\Omega}_1\omega)^2\}^{1.5}} \tag{24}$$

and

$$\frac{\partial H_{1ij}}{\partial\omega} = \frac{2\phi_{1i}\phi_{1j}\{\Omega_1^2(1 - 2\zeta_1^2) - \omega^2\}}{m_1\{(\Omega_1^2 - \omega^2)^2 + (2\zeta_1\Omega_1\omega)^2\}^{1.5}} \tag{25}$$

The sensitivity for both high- and low-stiffness states as Eqs. (24) and (25) must satisfy the following relationships (see Appendix):

$$(\partial\hat{H}_{1ij}/\partial\omega)(\partial H_{1ij}/\partial\omega) < 0, \qquad (\omega_1 < \omega < \omega_2) \tag{26a}$$

$$(\partial\hat{H}_{1ij}/\partial\omega)(\partial H_{1ij}/\partial\omega) > 0, \qquad (\omega < \omega_1, \omega > \omega_2) \tag{26b}$$

and

$$(\partial\hat{H}_{1ij}/\partial\omega)(\partial H_{1ij}/\partial\omega) = 0, \qquad (\omega = \omega_1, \omega_2) \tag{26c}$$

where ω_1 and ω_2 are the resonance frequencies for the low- and high-stiffness states, which are known to be expressed by the following equations:

$$\omega_1 = \Omega_1\sqrt{1 - 2\zeta_1^2} \approx \Omega_1 \tag{27a}$$

and

$$\omega_2 = \hat{\Omega}_1\sqrt{1 - 2\hat{\zeta}_1^2} \approx \hat{\Omega}_1 \tag{27b}$$

Here, we assume that ζ^2, $\hat{\zeta}_1^2 \ll 1$ for lightly damped systems. Therefore, Eq. (26) can be rewritten as

$$(\partial\hat{H}_{1ij}/\partial\omega)(\partial H_{1ij}/\partial\omega) < 0, \qquad (\Omega_1 < \omega < \hat{\Omega}_1) \tag{28a}$$

$$(\partial\hat{H}_{1ij}/\partial\omega)(\partial H_{1ij}/\partial\omega) > 0, \qquad (\omega < \Omega_1, \omega > \hat{\Omega}_1) \tag{28b}$$

and

$$(\partial\hat{H}_{1ij}/\partial\omega)(\partial H_{1ij}/\partial\omega) = 0, \qquad (\omega = \Omega_1, \hat{\Omega}_2) \tag{28c}$$

Further, the following relationship should be satisfied for the derivatives of R_j with respect to the excitation frequency ω:

$$\partial R_j/\partial\omega > 0, \qquad (\bar{\omega}_1 < \omega < \bar{\omega}_2) \tag{29a}$$

$$\partial R_j/\partial\omega < 0, \qquad (\omega < \bar{\omega}_1, \omega > \bar{\omega}_2) \tag{29b}$$

and

$$\partial R_j/\partial\omega = 0, \qquad (\omega = \bar{\omega}_1, \bar{\omega}_2) \tag{29c}$$

where $\bar{\omega}_1$ and $\bar{\omega}_2$ ($\bar{\omega}_1 < \bar{\omega}_2$) are the two extrema of R_j.

On the other hand, the derivative of R_j can be theoretically obtained using Eq. (14) as

$$\frac{\partial R_j}{\partial\omega} = 2\left\{\frac{(\omega^3 - \Omega_1^2\omega + \zeta_1^2\Omega_1^2\omega)B - (\omega^3 - \hat{\Omega}_1^2\omega + \hat{\zeta}_1^2\hat{\Omega}_1^2\omega)A}{\sqrt{AB^3}}\right\} \tag{30}$$

where A and B are given by

$$A = \left(\Omega_1^2 - \omega^2\right)^2 + (2\zeta_1\Omega_1\omega)^2 \quad \text{and}$$
$$B = \left(\hat{\Omega}_1^2 - \omega^2\right)^2 + (2\hat{\zeta}_1\hat{\Omega}_1\omega)^2 \tag{31}$$

Then, the two excitation frequencies yielding the extrema of R_j are given by $\partial R_j/\partial\omega = 0$, by use of which one can obtain the following equation:

$$\omega^4 - \left(\hat{\Omega}_1^2 + \Omega_1^2 + 2\zeta_1^2\Omega_1^2\right)\omega^2 + \hat{\Omega}_1^2\Omega_1^2 - \zeta_1^2\Omega_1^2\left(\hat{\Omega}_1^2 + \Omega_1^2\right) = 0 \tag{32}$$

Again, under the assumption that $\zeta_1^2 \ll 1$, Eq. (32) can be rewritten as

$$\omega^4 - \left\{\hat{\Omega}_1^2 + \Omega_1^2\right\}\omega^2 + \hat{\Omega}_1^2\Omega_1^2 = 0 \tag{33}$$

Finally, the solutions of Eq. (33) are easily calculated as $\omega^2 = \Omega_1^2$, $\hat{\Omega}_1^2$. Accordingly, in Eqs. (29), $\bar{\omega}_1 = \Omega_1$ and $\bar{\omega}_2 = \hat{\Omega}_1$. Thus, Eq. (29) is rewritten as

$$\partial R_j/\partial\omega > 0, \qquad (\Omega_1 < \omega < \hat{\Omega}_1) \tag{34a}$$

$$\partial R_j/\partial\omega < 0, \qquad (\omega < \Omega_1, \omega > \hat{\Omega}_1) \tag{34b}$$

and

$$\partial R_j/\partial\omega = 0, \qquad (\omega = \Omega_1, \hat{\Omega}_1) \tag{34c}$$

By using the sensitivity relations, Eqs. (28) and (34), one can select a feasible or acceptable value from the two candidates in Eq. (22). It should be noted that this approach requires the calculation of the derivatives of $\hat{H}_{1ij}$, H_{1ij}, and R_j; consequently, at least two different sets of R_j and $\hat{H}_{1ij}$, H_{1ij} corresponding to two different excitation frequencies are required. For example,

$$\left.\frac{\partial\hat{H}_{1ij}}{\partial\omega}\right|_{\omega=\omega_k} \approx \frac{1}{2}\left\{\frac{\hat{H}_{1ij}(\omega_{k+1}) - \hat{H}_{1ij}(\omega_k)}{\omega_{k+1} - \omega_k}\right\}, \qquad (k = 1) \tag{35a}$$

$$\left.\frac{\partial\hat{H}_{1ij}}{\partial\omega}\right|_{\omega=\omega_k} \approx \frac{1}{2}\left\{\frac{\hat{H}_{1ij}(\omega_{k+1}) - \hat{H}_{1ij}(\omega_{k-1})}{\omega_{k+1} - \omega_{k-1}}\right\} \tag{35b}$$
$$(k = 2, \ldots, N-1)$$

and

$$\left.\frac{\partial\hat{H}_{1ij}}{\partial\omega}\right|_{\omega=\omega k} \approx \frac{1}{2}\left\{\frac{\hat{H}_{1ij}(\omega_k) - \hat{H}_{1ij}(\omega_{k-1})}{\omega_k - \omega_{k-1}}\right\}, \qquad (k = N) \tag{35c}$$

where N is the number of different excitation frequencies. Note that for $k = 2, \ldots, N-1$, a central difference approximation of the derivative is used as Eq. (35b). For the cases of $\partial H_{1ij}/\partial\omega$ and $\partial R_j/\partial\omega$, the same approximation is used to calculate their derivatives.

When the correct value is selected on the basis of the sensitivity properties, the natural frequency for the high-stiffness state is calculated by substituting the identified Ω_1 into Eq. (17) as the following equation:

$$\hat{\Omega}_1 = \sqrt{R_\Omega}\,\Omega_1 \tag{36}$$

Thus far, this study has proposed the estimation algorithms for identifying the first natural frequencies for the high- and low-stiffness states; these frequencies are expressed by Eqs. (22) and (36), respectively. The algorithm is straightforward because it only needs to observe the frequency response amplitudes $\hat{H}_{1ij}$ and H_{1ij} for estimating R_j under stationary excitation. Excitation force data need not be observed because the algorithms do not require the excitation data to implement the identification.

Because a stationary vibration for unknown periodic excitation is assumed to be observed, for more general disturbances, such as nonstationary excitation force and impact force, further investigation must be carried out. However, the present approach is useful for specific situations in which space structures are subject to unknown stationary disturbances.

3. *Summary of Estimation Algorithm*

In summary, the proposed estimation algorithm is described as follows:

1) Calculate R_Ω using Eq. (17) from the natural frequencies before mass variation $\hat{\Omega}_1^*$ and Ω_1^*.

2) Measure a set of $\hat{H}_{1ij}$ and H_{1ij} under stationary sinusoidal excitation whose frequency is ω_k.

3) Calculate $\tilde{R}_j$ from $\hat{H}_{1ij}$ and H_{1ij} using Eq. (18).

4) Calculate the approximated sensitivities $\partial\hat{H}_{1ij}/\partial\omega$, $\partial H_{1ij}/\partial\omega$, and $\partial R_j/\partial\omega$ from the excitation frequency ω_k and the measured $\hat{H}_{1ij}$, H_{1ij}, and $\tilde{R}_j$. [This step requires at least two sets of the excitation frequencies ω_{k-1} and ω_{k+1}. and the frequency response amplitudes for calculating the sensitivities using Eq. (35).]

5) Calculate Ω_1 by substituting R_Ω, ζ_1, $\tilde{R}_j$, and ω into Eq. (22).

6) Calculate $\hat{\Omega}_1$ by substituting Ω_1 obtained by step 5 into Eq. (36).

7) Select the feasible solutions $\hat{\Omega}_1$ and Ω_1 that satisfy the sensitivity requirements, Eqs. (28) and (34).

IV. Experiments

In this section, we present the experimental results of the identification of the first modal frequency of the 10-bay truss structure shown in Fig. 2 to demonstrate the proposed procedures. Figure 3 shows a photograph of the 10-bay truss. Although the general formulation of the proposed method has been presented for the case when multiple piezoelectric actuators can be employed for changing the stiffness of the truss structure, we carry out the identification by the single actuator for simplicity. Using an electromagnetic exciter, the frequency response amplitudes of the truss for the low- and high-stiffness states are measured, and then the change ratio of these amplitudes is calculated. The obtained change ratio of the frequency response amplitude is finally used to identify the first natural frequency of the truss by the proposed method.

In the experiments, an additional mass (see Fig. 4) attached at the tip of the truss is used to simulate an on-orbit change in the structural configuration or docking. The additional mass is used just to demonstrate the applicability of the method to two different structures whose first natural frequencies are different. Thus, the additional mass and its location are determined so that the first natural frequencies of these structures can be obtained. It should again noted that only stiffness control with piezoelectric actuator is adopted to implement the proposed method. The change in the modal mass during the stiffness control is neglected.

The experimental setup consists of the 10-bay truss structure with a piezoelectric actuator (NEC/TOKIN ASB171C801NP0; see

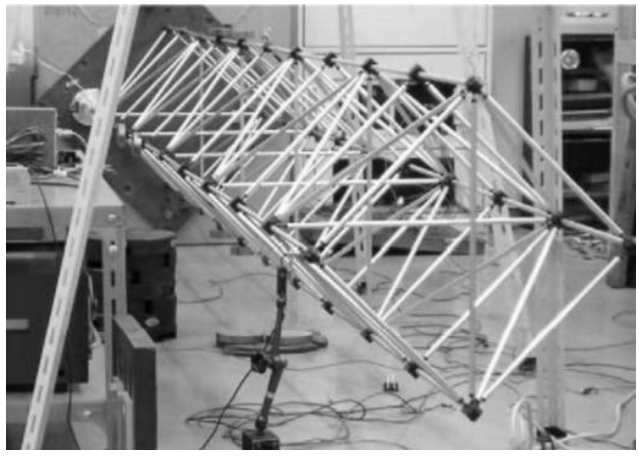

Fig. 3 Photograph of 10-bay truss structure for experiments.

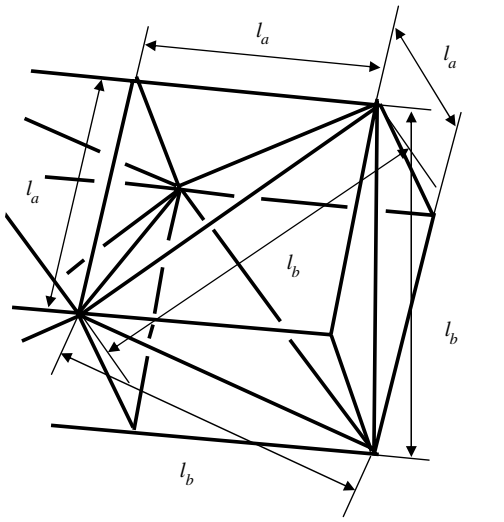

a)

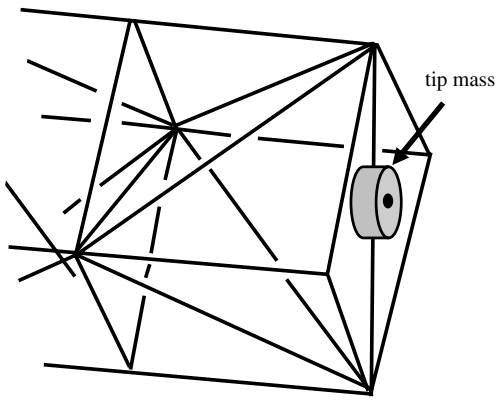

b)

Fig. 4 Definition of a) axial and diagonal members, b) additional mass as intentional modeling error $\Delta M = 1.86$ kg at tip of truss.

Fig. 1), an eddy current displacement sensor (KEYENCE, EX201-305), laser displacement sensor (KEYENCE, LC-2430), control unit for laser displacement sensor (KEYENCE, LC-2430), noncontact electromagnetic coil exciter, analog/digital (A/D) converter, and D/A converter. In Fig. 2, outputs 1 and 2 correspond to the outputs of the eddy current displacement sensor and laser displacement sensor, respectively. The properties of the truss are listed in Table 1. The materials of truss members and nodes are aluminum alloy and chrome molybdenum steel, respectively. Further, the properties of the piezoelectric device are shown in Table 1. From Table 1, it can be observed that the axial stiffness of the variable member can be changed by approximately 13% because the constant stiffness $k_p = 5.75 \times 10^6$ N/m and the additional stiffness for the high-stiffness state $\Delta k_p = 7.72 \times 10^5$ N/m.

Table 1 Properties of 10-bay truss structure with piezoelectric device

Constant-charge stiffness, k_p, N/m	5.75×10^6
Piezoelectric constant, b_p, N/C	2.57×10^5
Constant-elongation capacitance, C_p, F	1.17×10^{-5}
Length of axial members, l_a, m	0.38
Length of diagonal members, l_b, m	0.54
Mass of axial members, m_a, g	35.7
Mass of diagonal members, m_b, g	46.3
Mass of node joints, m_c, g	67.9
Stiffness of each member, EA, N	1.99×10^6
Point masses at third and fourth bay, m_d, kg	0.5
Stiffness variation, $\Delta k_p = b_p^2 C_p^S$, N/m	7.72×10^5
Mass of piezoelectric actuator, m_p, g	93.0

Although the vibration properties of the 10-bay truss structure have already been studied in literature [34,36], we have performed preliminary experiments to verify the exact value of the first bending natural frequency of the test truss. By using the noncontact electromagnetic coil exciter, a stationary sinusoidal excitation is applied to the truss at the location shown in Fig. 2. The excitation frequency is varied from 10 to 12 Hz in steps of 0.01 Hz. Then, we obtain the resonance frequency for the high- and low-stiffness states as the frequency with the largest amplitude. For the truss without additional mass, the first bending natural frequencies are $\hat{\Omega}_1 = 11.30$ Hz and $\Omega_1 = 11.15$ Hz for the high- and low-stiffness states, respectively. For the truss with additional mass, the corresponding natural frequencies are $\hat{\Omega}_1 = 8.66$ Hz and $\Omega_1 = 8.54$ Hz for the high- and low-stiffness states, respectively. These values are used as the exact values, which are compared with those obtained by the proposed methodology. Further, we have observed the change ratio of the first mode shape ϕ_{11}/ϕ_{12}, which is the ratio of the displacements between outputs 1 and 2, was approximately 1% or less. From this result, the assumption of ignoring the change in the mode shape due to the stiffness control has been satisfied sufficiently.

In the next section, we present experimental demonstrations that show the identification of the first bending natural frequency. The results of the identification for two different cases are shown: one is the identification for the truss with the additional mass, $\Delta M = 1.86$ kg (case 1), and the other is that without the additional mass (case 2), where the additional mass is shown in Fig. 4.

A. Results with Additional Mass (Case 1)

Figure 5 shows the frequency response amplitude obtained by preliminary experiments. The frequency response amplitudes for the high- and low-stiffness states are obtained from the amplitude of each excitation frequency. These results are measured by stationary forced vibration using the electromagnetic exciter, whose excitation frequency is varied in steps of 0.02 Hz. The minimum and maximum excitation frequencies are 8.50 and 8.70 Hz, respectively. These frequency bands are determined so that the excitation frequency includes the first bending natural frequencies for the high- and low-stiffness states.

Figure 6 shows the change ratio of the frequency response amplitude defined in Eq. (14). The sample vibration data used to obtain the frequency response amplitude for output 1 are shown in Fig. 7, for which the excitation frequency is 8.54 Hz. It should be noted that the phases of all vibration data are different, and they are not used for the identification. Only the changes in the amplitude and its sensitivity to the vibration shown in these spectra are used for the identification.

To select the feasible solution given by Eq. (22), the evaluation of the sensitivities of H_{1ij} and R_j requires at least two different excitation frequencies for calculating the approximated derivatives expressed in Eqs. (28) and (34).

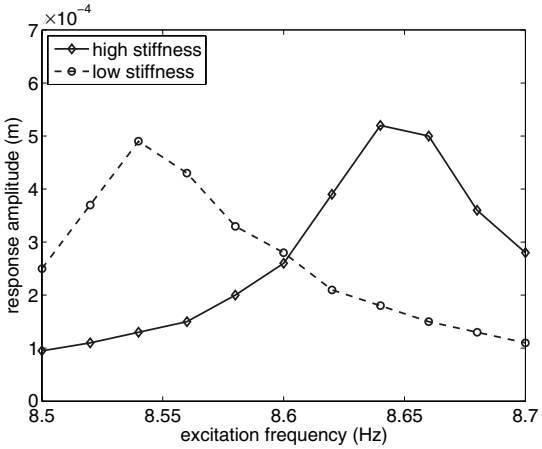

Fig. 5 Frequency response amplitudes for the high- and low-stiffness states for case 1 and output 1.

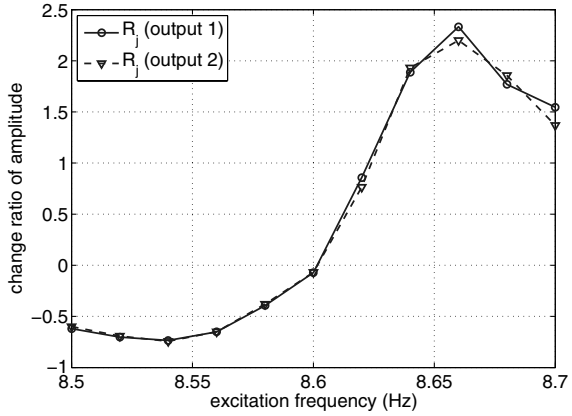

Fig. 6 Change ratio of frequency response amplitude for case 1; R_j for outputs 1 and 2 shown in Fig. 2.

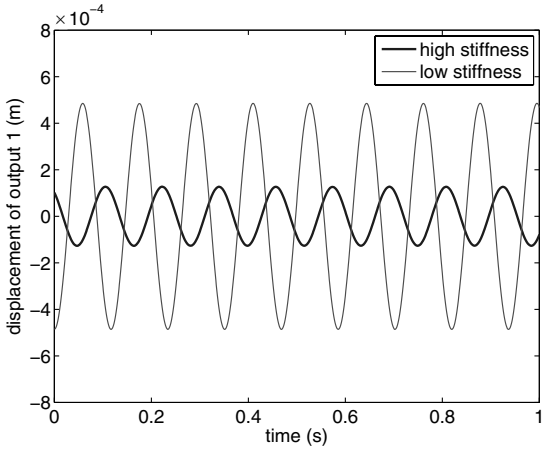

Fig. 7 Stationary vibration data for case 1 and output 1 with sinusoidal excitation frequency of 8.54 Hz.

In literature, the damping ratio for the first mode of the 10-bay truss structure has been expressed as $\zeta_1 = 0.0036$ [34,36], where the value is estimated from the free vibration data of the first mode. Although the truss used in this study is the same as that used in the literature, the damping ratio may change slightly because of the change in testing environment. Further, in literature, typical damping ratios of the lower vibration modes for space structures are approximately 0.005–0.01 [8]. According to these literatures, we have used three different damping ratios that are substituted into Eq. (22) to identify the first natural frequency Ω_1. These ratios are $\zeta_1 = 0.003$, 0.005, and 0.008. Once Ω_1 is obtained, it is substituted into Eq. (36) to estimate $\hat{\Omega}_1$.

Figures 8a–8c show the results of estimation of the first natural frequencies $\hat{\Omega}_1$ and Ω_1 for case 1. The change ratio R_j (output 1) in Fig. 6 is used as $\tilde{R}_j$ in the estimation. In Figs. 8a–8c, "exact (high stif.)" represents the exact natural frequency obtained by the preliminary experiments for the high-stiffness state, that is, 8.66 Hz. Further, "exact (low stif.)" represents the exact natural frequency for the low-stiffness state, that is, 8.54 Hz. On the other hand, "id. (high stif.)" and "id. (low stif.)" represent the identified frequencies $\hat{\Omega}_1$ and Ω_1 for high- and low-stiffness states, respectively. $\hat{\Omega}_1$ is obtained by Eq. (36), whereas Ω_1 is obtained by Eq. (22), respectively.

Figure 8 shows that the deviation of the identified natural frequency for $\zeta_1 = 0.005$ is the smallest among the three cases. The deviation of the identified natural frequencies for $\zeta_1 = 0.008$ shows the largest fluctuation. From Fig. 8, it can be observed that the

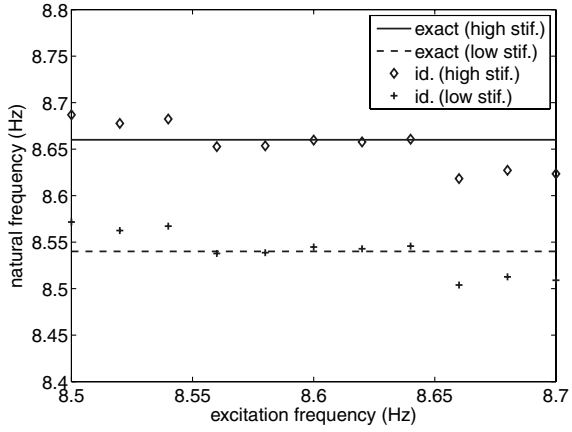

a) $\zeta_1 = 0.003$

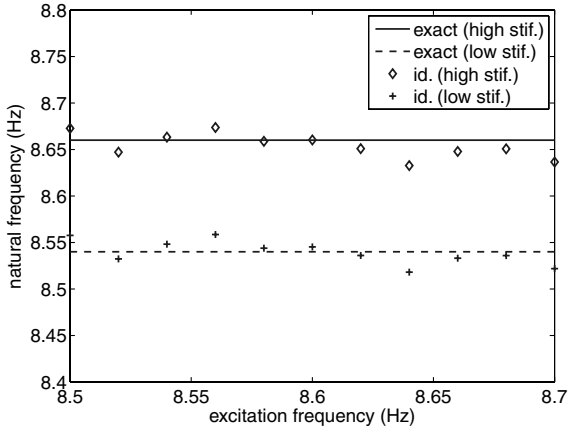

b) $\zeta_1 = 0.005$

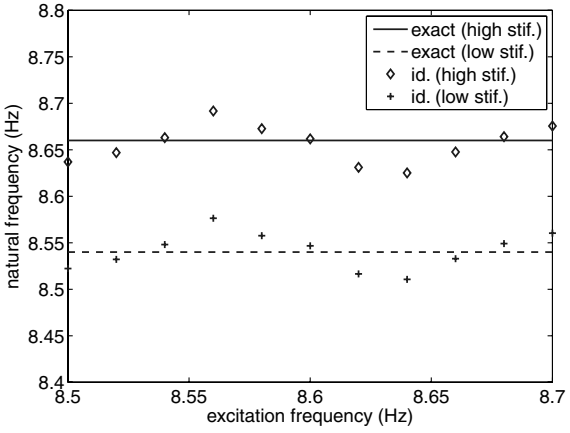

c) $\zeta_1 = 0.008$

Fig. 8 Estimated natural frequencies for high- and low-stiffness states for case 1.

identification error is clearly dependent on the damping ratio and excitation frequency. The factors causing such phenomena will be discussed later by carrying out sensitivity analysis of the change ratio R_j with respect to the damping ratio ζ_1.

B. Results Without Additional Mass (Case 2)

In the next experiment, the first natural frequency for case 2, in which the additional mass is not attached to the truss, is identified by the proposed method. Figure 9 shows the frequency response amplitude obtained by preliminary experiments. The excitation frequency is changed from 11.00 to 11.40 Hz in steps of 0.02 Hz, which includes the first bending natural frequencies for both the high- and low-stiffness states. Figure 10 shows the change ratio of the frequency response amplitude defined in Eq. (14). The stationary vibration data for output 1 used to obtain the frequency response amplitude are shown in Fig. 11. The amplitude for the high-stiffness state is greater than that for the low-stiffness state because the natural frequency of the high-stiffness state is closer to the excitation frequency.

Figures 12a–12c show the results of the estimation of the first natural frequency for case 2 using the three different damping values. The change ratio R_j (output 1) in Fig. 10 is used as $\tilde{R}_j$ in the estimation. It is shown in Fig. 12 that the deviation of the identified natural frequency in the results for $\zeta_1 = 0.005$ is the smallest among the three cases. In particular, the results for $\zeta_1 = 0.008$ deviate more significantly than those for other ζ_1 values. The identification error and its deviation observed in Fig. 12 are qualitatively similar to the those observed for case 1.

In the following section, we discuss the error factors on the basis of sensitivity analyses.

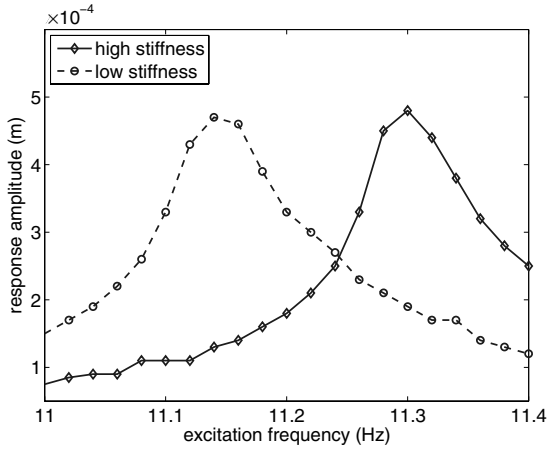

Fig. 9 Frequency response amplitudes for high- and low-stiffness states for case 2 and output 1.

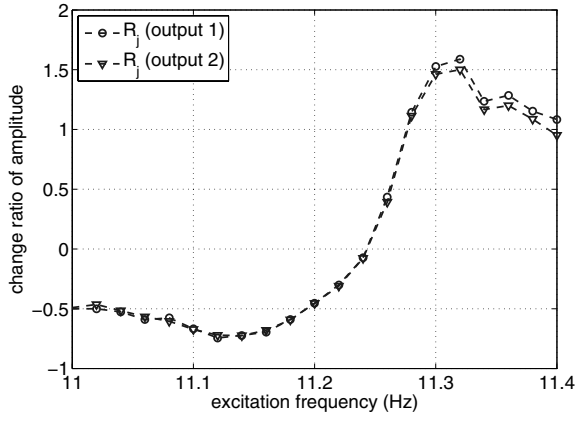

Fig. 10 Change ratio of frequency response amplitude for case 2; R_j for outputs 1 and 2 shown in Fig. 2.

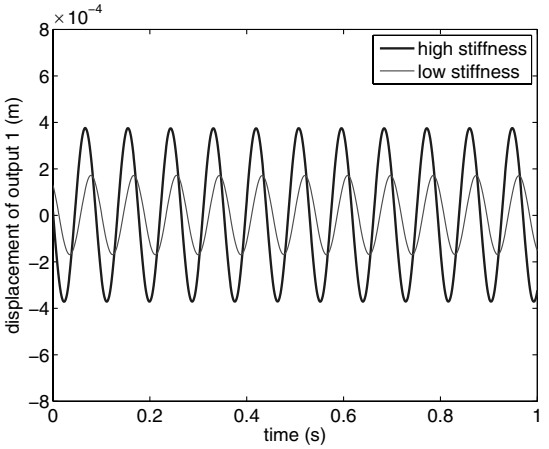

Fig. 11 Stationary vibration data for case 2 and output 1 with sinusoidal excitation frequency of 11.34 Hz.

C. Discussion on Estimation Accuracy

To analyze the reason for the identification error that appears to depend on the excitation frequency ω and damping ratio ζ_1, we carried out a theoretical analysis of the sensitivity of R_j with respect to the damping ratio ζ_1. The gradient of R_j with respect to ζ_1 is derived by differentiating the right-hand side of Eq. (20) with ζ_1 as

$$\frac{\partial R_j}{\partial \zeta_1} = \frac{4\zeta_1 \Omega_1^2 \omega^2 (\hat{\Omega}_1^2 - \Omega_1^2)(\hat{\Omega}_1^2 + \Omega_1^2 - 2\omega^2)}{\sqrt{(\Omega_1^2 - \omega^2)^2 + (2\zeta_1 \Omega_1 \omega)^2}\{(\hat{\Omega}_1^2 - \omega^2)^2 + (2\zeta_1 \Omega_1 \omega)^2\}^{1.5}} \tag{37}$$

From Eq. (37), it is observed that when the excitation frequency ω is close to $\sqrt{(\hat{\Omega}_1^2 + \Omega_1^2)/2}$, the right-hand side of Eq. (37) becomes zero, that is, R_j is independent of the damping ratio. Thus, it is expected that the identification error reduces less when the excitation frequency is close to $\sqrt{(\hat{\Omega}_1^2 + \Omega_1^2)/2}$. Even when the damping ratio substituted into Eq. (22) has some error, it may not affect the identification of the natural frequency. In fact, these properties are clearly observed in the experimental results shown in Figs. 8 and 12. The specific excitation frequency for which $\partial R_j / \partial \zeta_1 = 0$ is 8.60 Hz for case 1 and 11.23 Hz for case 2. The deviation of the identified natural frequencies around these excitation frequencies are less than those of the identified natural frequencies around other frequencies. Therefore, we may conclude that the reason for the deviation of the identification is the sensitivity of R_j.

In addition to the aforementioned theoretical analysis, we have also calculated R_j and its sensitivity for case 1 and case 2 using Eq. (37), in which $\zeta_1 = 0.005$ is substituted. For case 1, $\hat{\Omega}_1 = 8.66$ and $\Omega_1 = 8.54$ are substituted into Eq. (37), whereas for case 2, $\hat{\Omega}_1 = 11.30$ and $\Omega_1 = 11.15$ are substituted into Eq. (37).

Figure 13 shows the results of the calculation of the sensitivity for each case. It is indicated that large extrema exist around 8.65 Hz for case 1 shown in Fig. 13a and around 11.30 Hz shown in Fig. 13b. Further, small extrema are observed around 8.55 Hz for case 1 shown in Fig. 13a and around 11.15 Hz shown in Fig. 13b.

Moreover, Fig. 14 shows the relationship between R_j and ζ_1, which is calculated substituting ζ_1, $\hat{\Omega}_1$, and Ω_1 into Eq. (20). Two extrema are found in each curve in Fig. 14. Similar extrema are appeared in the experimental results shown in Figs. 8c and 12c. Therefore, it is concluded that the large identification error for the specific excitation frequency is due to the large sensitivity of R_j with respect to the damping ratio.

Although we can explain the reason for the identification error by analyzing the sensitivity of R_j, other error factors may exist in the laboratory environment, such as measurement noise and nonstationary ambient disturbances. Further, we have neglected the contribution of the higher vibration modes in the study. We should

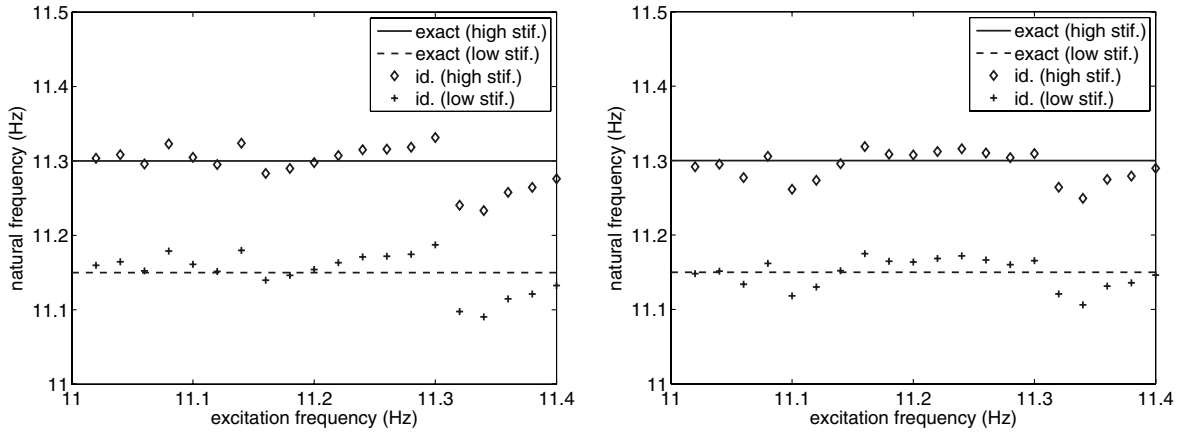

a) ζ_1=0.003 **b) ζ_1=0.005**

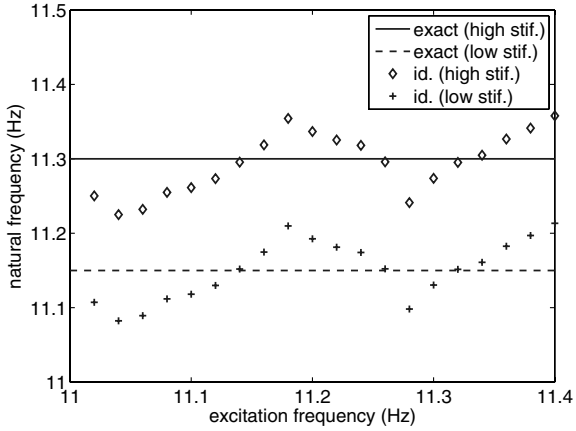

c) ζ_1=0.008

Fig. 12 Estimated natural frequencies for high- and low-stiffness states for case 2.

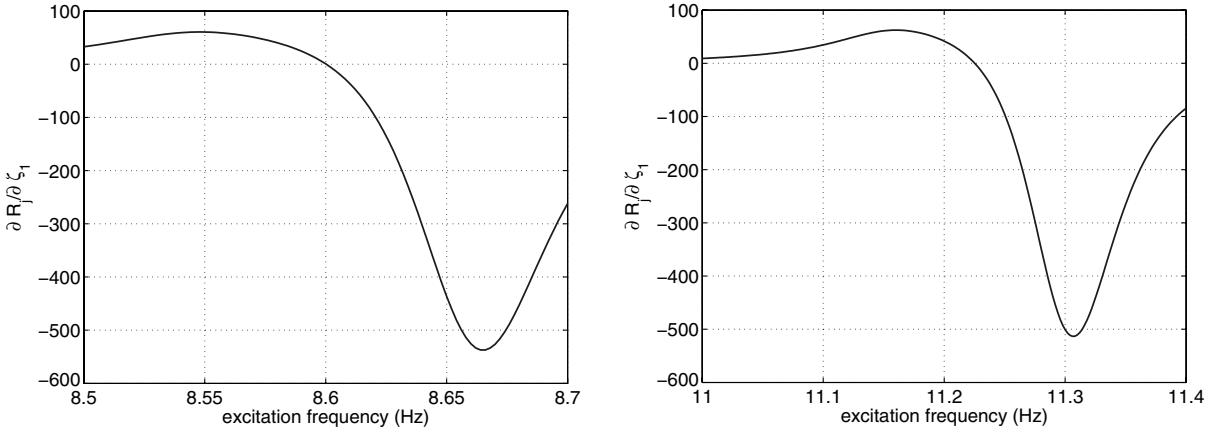

a) Case 1 **b) Case 2**

Fig. 13 Sensitivity of change ratio R_j with respect to damping ratio ζ_1 ($\zeta_1 = 0.005$).

further investigate the effect of these factors for improving the accuracy of identification.

For realistic on-orbit identification of space structures, noncontact displacement sensors, such as laser displacement sensors that have a high resolution, may not be easily employed to measure their frequency response amplitude. In this case, accelerometers can be employed to measure the frequency response amplitude. Further, averaging of the frequency response amplitude should be implemented before calculating the natural frequency by the proposed methodology, specifically for vibration data of low signal-to-noise ratio. Thus, the proposed method is applicable to the practical use in space environment by employing other types of sensors and the averaged frequency response amplitude.

V. Conclusions

This study has investigated the possibility of the identification of the fundamental natural frequency of truss structures on the basis of the change in the frequency response amplitude by using variable-stiffness devices embedded in a specific truss member. The use of the change ratio of the frequency response amplitude is described specifically for the on-orbit modal identification under conditions

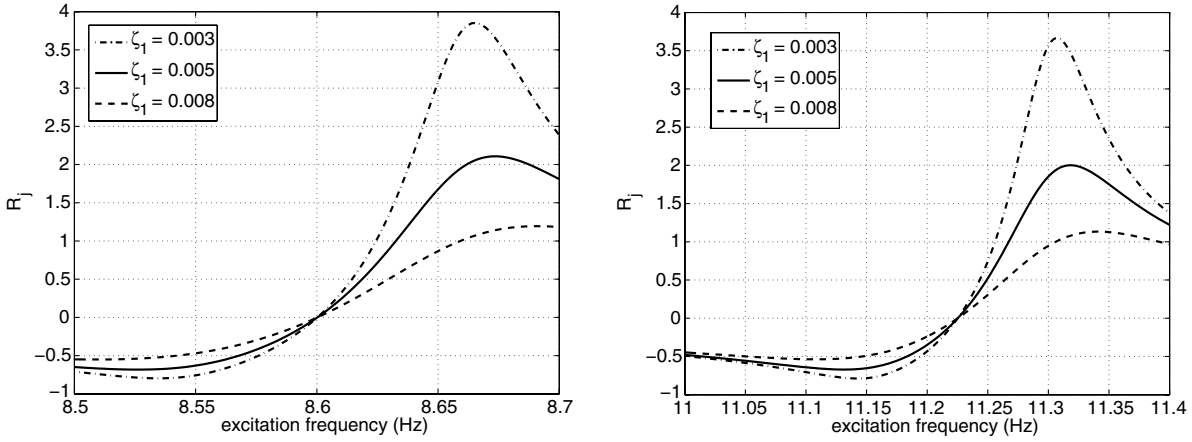

a) Case 1 **b) Case 2**

Fig. 14 Change ratio R_j for three different damping ratios.

where only output data are available and the excitation force cannot be measured in orbit. To demonstrate the proposed procedures, we have provided experimental demonstrations for identifying the first bending natural frequency of the 10-bay truss structure with a piezoelectric actuator that changes the stiffness, resulting in two different states (i.e., high- and low-stiffness states).

The experimental results show that the first bending natural frequency is identified with acceptable accuracy. However, in the experiments, the identification shows a deviation that depends on the excitation frequency and damping ratio. To analyze the reason for this deviation, we have carried out theoretical and numerical analyses of the error factors. From the theoretical analyses, it is found that the identification accuracy is independent of the accuracy of the damping ratio when a specific excitation frequency, derived from the natural frequencies for the high- and low-stiffness states, is used for the identification. Further, using an excitation frequency close to the extrema of the sensitivity of the change ratio in the frequency response amplitude increases the identification error when the damping ratio has some error. Although the estimation performance is dependent on the excitation frequency, the potential of the present approach is verified experimentally.

Finally, it should be noted that the proposed method is formulated assuming that the contribution of the higher modes and change in the mode shape and the modal mass, due to the change in the stiffness by the piezoelectric actuators, are neglected. For example, if the multiple modes are not well separated because of high-modal density, the multiple modes must be taken into account for formulating the change ratio of the frequency response amplitudes. The applicability of the proposed method to practical structures will be investigated in the future by considering these aspects.

Appendix: Proof of Equations

In the Appendix, the proof of each equation in Eq. (26) is presented.

Equations (24) and (25) are rewritten using ω_1 and ω_2, which were expressed by Eqs. (27a) and (27b):

$$\frac{\partial \hat{H}_{1ij}}{\partial \omega} = \frac{2\hat{\phi}_{1i}\hat{\phi}_{1j}\{\omega_2^2 - \omega^2\}}{\hat{m}_1\{(\hat{\Omega}_1^2 - \omega^2)^2 + (2\hat{\zeta}_1\hat{\Omega}_1\omega)^2\}^{1.5}} > 0, \qquad (\omega < \omega_2) \tag{A1}$$

and

$$\frac{\partial H_{1ij}}{\partial \omega} = \frac{2\phi_{1i}\phi_{1j}\{\omega_1^2 - \omega^2\}}{m_1\{(\Omega_1^2 - \omega^2)^2 + (2\zeta_1\Omega_1\omega)^2\}^{1.5}} < 0, \qquad (\omega_1 < \omega) \tag{A2}$$

The following relationship can be derived from Eqs. (A1) and (A2) for $\omega_1 < \omega < \omega_2$:

$$\left(\frac{\partial \hat{H}_{1ij}}{\partial \omega}\right)\left(\frac{\partial H_{1ij}}{\partial \omega}\right) < 0 \tag{A3}$$

Thus, Eq. (26a) is clearly satisfied. Further, for excitation frequency $\omega < \omega_1$, $(\omega_1 < \omega_2)$, the following relationships are obtained:

$$\frac{\partial \hat{H}_{1ij}}{\partial \omega} = \frac{2\hat{\phi}_{1i}\hat{\phi}_{1j}\{\omega_2^2 - \omega^2\}}{\hat{m}_1\{(\hat{\Omega}_1^2 - \omega^2)^2 + (2\hat{\zeta}_1\hat{\Omega}_1\omega)^2\}^{1.5}} > 0 \tag{A4}$$

and

$$\frac{\partial H_{1ij}}{\partial \omega} = \frac{2\phi_{1i}\phi_{1j}\{\omega_1^2 - \omega^2\}}{m_1\{(\Omega_1^2 - \omega^2)^2 + (2\zeta_1\Omega_1\omega)^2\}^{1.5}} > 0 \tag{A5}$$

Thus, the following relationship is derived:

$$\left(\frac{\partial \hat{H}_{1ij}}{\partial \omega}\right)\left(\frac{\partial H_{1ij}}{\partial \omega}\right) > 0, \qquad (\omega < \omega_1) \tag{A6}$$

Furthermore, for excitation frequency $\omega > \omega_2$,

$$\frac{\partial \hat{H}_{1ij}}{\partial \omega} = \frac{2\hat{\phi}_{1i}\hat{\phi}_{1j}\{\omega_2^2 - \omega^2\}}{\hat{m}_1\{(\hat{\Omega}_1^2 - \omega^2)^2 + (2\hat{\zeta}_1\hat{\Omega}_1\omega)^2\}^{1.5}} < 0 \tag{A7}$$

and

$$\frac{\partial H_{1ij}}{\partial \omega} = \frac{2\phi_{1i}\phi_{1j}\{\omega_1^2 - \omega^2\}}{m_1\{(\Omega_1^2 - \omega^2)^2 + (2\zeta_1\Omega_1\omega)^2\}^{1.5}} < 0 \tag{A8}$$

Then, the following relationship is also derived:

$$\left(\frac{\partial \hat{H}_{1ij}}{\partial \omega}\right)\left(\frac{\partial H_{1ij}}{\partial \omega}\right) > 0, \qquad (\omega > \omega_2) \tag{A9}$$

Hence, Eq. (26b) is verified by Eqs. (A6) and (A9). For excitation frequency $\omega = \omega_1$,

$$\frac{\partial H_{1ij}}{\partial \omega} = \frac{2\phi_{1i}\phi_{1j}\{\omega_1^2 - \omega^2\}}{m_1\{(\Omega_1^2 - \omega^2)^2 + (2\zeta_1\Omega_1\omega)^2\}^{1.5}} = 0 \tag{A10}$$

Further, for excitation frequency $\omega = \omega_2$,

$$\frac{\partial \hat{H}_{1ij}}{\partial \omega} = \frac{2\hat{\phi}_{1i}\hat{\phi}_{1j}\{\omega_2^2 - \omega^2\}}{\hat{m}_1\{(\hat{\Omega}_1^2 - \omega^2)^2 + (2\hat{\zeta}_1\hat{\Omega}_1\omega)^2\}^{1.5}} = 0 \tag{A11}$$

are satisfied; therefore, Eq. (26c) is derived as

$$\left(\frac{\partial \hat{H}_{1ij}}{\partial \omega}\right)\left(\frac{\partial H_{1ij}}{\partial \omega}\right) = 0, \qquad (\omega = \omega_1, \omega_2) \tag{A12}$$

Acknowledgments

The authors thank Junjiro Onoda and Kanjuro Makihara in the Space Structure and Materials Department at the Institute of Space and Astronautical Sciences/Japan Aerospace Exploration Agency for their support. The authors also acknowledge the financial support provided by the Society for Promotion of Space Sciences.

References

[1] Rajaram, S., and Junkins, J. L., "Identification of Vibrating Flexible Structures," *Journal of Guidance, Control, and Dynamics*, Vol. 8, No. 4, 1985, pp. 463–470.

[2] Okuma, M., Heylen, W., Matsuoka, H., and Sas, P., "Identification and Prediction of Frame Structure Dynamics by Spatial Matrix Identification Method," *Journal of Vibration and Acoustics*, Vol. 123, No. 3, 2001, pp. 390–394. doi:10.1115/1.1377020

[3] Alvin, K. F., Robertson, A. N., Reich, G. W., and Park, K. C., "Structural System Identification: From Reality to Models," *Computers and Structures*, Vol. 81, No. 12, 2003, pp. 1149–1176. doi:10.1016/S0045-7949(03)00034-8

[4] Chen, J. C., and Fanson, J. L., "System Identification Test Using Active Members," *AIAA Journal*, Vol. 29, No. 4, 1991, pp. 633–640.

[5] Chen, J. C., and Garba, A., "On-Orbit Damage Assessment for Large Space Structures," *AIAA Journal*, Vol. 26, No. 9, 1988, pp. 1119–1126.

[6] Kammer, D. C., "Sensor Placement for On-Orbit Modal Identification and Correlation of Large Space Structures," *Journal of Guidance, Control, and Dynamics*, Vol. 14, No. 2, 1991, pp. 251–259.

[7] Anthony, T., and Anderson, G., "On-Orbit Modal Identification of the Hubble Space Telescope," *Proceedings of the American Control Conference*, Inst. of Electrical and Electronics Engineers, New York, June 1995, pp. 402–406.

[8] Adachi, S., Yamaguchi, I., Kida, T., Sekiguchi, T., Yamada, K., and Chida, Y., "On-Orbit System Identification Experiments on Engineering Test Satellite ETS-VI," *Control Engineering Practice*, Vol. 7, No. 7, 1999, pp. 831–841. doi:10.1016/S0967-0661(99)00032-5

[9] Kammer, D. C., and Stelzner, A. D., "Structural Identification of Mir Using Inverse System Dynamics and Mir/Shuttle Docking Data," *Journal of Vibration and Acoustics*, Vol. 123, No. 2, 2001, pp. 230–237. doi:10.1115/1.1355030

[10] Boucher, R. L., "Identification and Mitigation of Low-Frequency Vibration Sources on Space Station," *Dynamics Specialists Conference*, AIAA Paper 96-1205, 1996.

[11] Schenk, A., and Pappa, R. S., "Practical Aspects of On-Orbit Modal Identification Using Free-Decay Data," *Journal of Spacecraft and Rockets*, Vol. 29, No. 2, 1992, pp. 264–270.

[12] Peeters, B., and Roeck, G., "Reference-Based Stochastic Subspace Identification for Output-Only Modal Analysis," *Mechanical Systems and Signal Processing*, Vol. 13, No. 6, 1999, pp. 855–878. doi:10.1006/mssp.1999.1249

[13] Juang, J., and Pappa, R. S., "Eigensystem Realization Algorithm for Modal Parameter Identification and Model Reduction," *Journal of Guidance, Control, and Dynamics*, Vol. 8, No. 5, 1985, pp. 620–627.

[14] Ljung, L., *System Identification: Theory for the User*, 2nd ed., Prentice–Hall, Englewood Cliffs, NJ, 1999.

[15] McKelvey, T., Akcay, H., and Ljung, L., "Subspace-Based Multivariable System Identification from Frequency Response Data," *IEEE Transactions on Automatic Control*, Vol. 41, No. 7, 1996, pp. 960–979. doi:10.1109/9.508900

[16] Pintelon, R., Schoukens, J., and Vandersteen, G., "Frequency Domain System Identification Using Arbitrary Signals," *IEEE Transactions on Automatic Control*, Vol. 42, No. 12, 1997, pp. 1717–1720. doi:10.1109/9.650025

[17] Goodzeit, N. E., and Phan, M. Q., "System Identification in the Presence of Completely Unknown Periodic Disturbances," *Journal of Guidance, Control, and Dynamics*, Vol. 23, No. 2, 2000, pp. 251–259.

[18] Brincker, R., Zhang, L., and Andersen, P., "Modal Identification of Output-Only Systems Using Frequency Domain Decomposition," *Smart Materials and Structures*, Vol. 10, No. 3, 2001, pp. 441–445. doi:10.1088/0964-1726/10/3/303

[19] Antoni, J., Garibarli, L., Marchesiello, S., and Sidhamed, M., "New Separation Techniques for Output-Only Modal Analysis," *Shock and Vibration*, Vol. 11, Nos. 3–4, 2004, pp. 227–242.

[20] Kim, B. H., Stubbs, N., and Park, T., "New Method to Extract Modal Parameters Using Output-Only Responses," *Journal of Sound and Vibration*, Vol. 282, Nos. 1–2, 2005, pp. 215–230. doi:10.1016/j.jsv.2004.02.026

[21] Lu, Z. R., and Law, S. S., "Identification of System Parameters and Input Force from Output Only," *Mechanical Systems and Signal Processing*, Vol. 21, No. 5, 2007, pp. 2099–2111. doi:10.1016/j.ymssp.2006.11.004

[22] Deraemaeker, A., Reymders, E., De Roeck, G., and Kullaa, J., "Vibration-Based Structural Health Monitoring Using Output-Only Measurement Under Changing Environment," *Mechanical Systems and Signal Processing*, Vol. 22, No. 1, 2008, pp. 34–56. doi:10.1016/j.ymssp.2007.07.004

[23] Ray, L. R., and Tian, L., "Damage Detection in Smart Structures Through Sensitivity Enhancing Feedback Control," *Journal of Sound and Vibration*, Vol. 227, No. 5, 1999, pp. 987–1002. doi:10.1006/jsvi.1999.2392

[24] Lew, J. S., "Optimal Controller Design for Structural Damage Detection," *Journal of Sound and Vibration*, Vol. 281, Nos. 3–5, 2005, pp. 799–813. doi:10.1016/j.jsv.2004.02.033

[25] Jung, H., and Park, Y., "Model Updating Using the Closed-Loop Natural Frequency," *Journal of Guidance, Control, and Dynamics*, Vol. 28, No. 1, 2005, pp. 20–28. doi:10.2514/1.4179

[26] Solbeck, J. A., and Ray, L. R., "Damage Identification Using Sensitivity-Enhancing Control and Identified Models," *Journal of Vibration and Acoustics*, Vol. 128, No. 2, 2006, pp. 210–220. doi:10.1115/1.2159037

[27] Jiang, L. J., Tang, J., and Wang, K. W., "Enhanced Frequency-Shift-Based Damage Identification Method Using Tunable Piezoelectric Transducer Circuitry," *Smart Materials and Structures*, Vol. 15, No. 3, 2006, pp. 799–808. doi:10.1088/0964-1726/15/3/016

[28] Senba, A., and Furuya, H., "Identifiability and Limitation of Self-Identification of Adaptive Structures by Variable Matrices Method," *Journal of the Japan Society for Aeronautical and Space Sciences* (in Japanese), Vol. 52, No. 609, 2004, pp. 479–486.

[29] Senba, A., and Furuya, H., "Implementation Algorithms for Self-Identification of Adaptive Structures with Variable Geometric Properties," *Mechanical Systems and Signal Processing*, Vol. 22, No. 1, 2008, pp. 1–14. doi:10.1016/j.ymssp.2007.05.002

[30] Senba, A., and Furuya, H., "Self-Identification Experiments Using Variable Inertia Systems for Flexible Beam Structures," *Journal of Vibration and Acoustics*, Vol. 130, No. 1, 2008, pp. 011006–011014. doi:10.1115/1.2776343

[31] Miura, K., and Furuya, H., "Adaptive Structure Concept for Future Space Applications," *AIAA Journal*, Vol. 26, No. 8, 1988, pp. 995–1002.

[32] Wada, B. K., "Adaptive Structures: An Overview," *Journal of Spacecraft and Rockets*, Vol. 27, No. 3, 1990, pp. 330–337.

[33] Onoda, J., Endo, T., Tamaoki, H., and Watanabe, N., "Vibration Suppression by Variable-Stiffness Members," *AIAA Journal*, Vol. 29, No. 6, 1991, pp. 977–983.

[34] Makihara, K., "Energy-Recycling Semi-Active Vibration Suppression of Space Structures," Ph.D. Dissertation, Univ. of Tokyo, Dept. of Aeronautical and Astronautics, Tokyo, 2003.

[35] Makihara, K., Onoda, J., and Menesugi, K., "Using Tuned Electrical Resonance to Enhance Bang–Bang Vibration Control," *AIAA Journal*, Vol. 45, No. 2, 2007, pp. 497–504. doi:10.2514/1.21736

[36] Makihara, K., Onoda, J., and Menesugi, K., "Low-Energy Consumption Hybrid Vibration Suppression Based on an Energy-Recycling Approach," *AIAA Journal*, Vol. 43, No. 8, 2005, pp. 1706–1715. doi:10.2514/1.14223

[37] Kosmatka, J. B., and Ricles, J. M., "Damage Detection in Structures by Modal Vibration Characterization," *Journal of Structural Engineering* Vol. 125, No. 12, 1999, pp. 1384–1392. doi:10.1061/(ASCE)0733-9445(1999)125:12(1384)

J. Wei
Associate Editor